Nanna Bjerregaard Pedersen*, Notburga Gierlinger and Lisbeth Garbrecht Thygesen

# Bacterial and abiotic decay in waterlogged archaeological *Picea abies* (L.) Karst studied by confocal Raman imaging and ATR-FTIR spectroscopy

**Abstract:** Waterlogged archaeological Norway spruce [*Picea abies* (L.) Karst] poles were studied by means of confocal Raman imaging (CRI) and attenuated total reflection Fourier transform infrared spectroscopy (ATR-FTIR) analysis to determine lignin and polysaccharide composition and distribution in the cell wall. The waterlogged archaeological wood (WAW) was submerged under anoxic conditions for approximately 400 years and solely decayed by erosion bacteria (EB). CRI showed that decayed tracheids contain a residual material (RM) with heterogeneous lignin distribution; within the same tracheid RM often contained regions with intensities lower than sound S2 layers up to intensity values as high as the compound middle lamella (CML). CRI revealed strong depletion of carbohydrates in RM which indicated that EB are able to utilise the carbohydrate fraction of the cell wall effectively. Raman bands assigned to lignin did not show any difference between RM and sound S2. This is a hint that EB do not modify the lignin structure. Sound WAW free from EB decay showed evidence of loss of acetyl groups in glucomannan, loss of un-conjugated ester linkages in the lignin-carbohydrate complexes between xylan and lignin, and minor oxidation of the lignin polymer compared to recent reference material. This is evidence for abiotic decay in the course of waterlogging.

**Keywords:** abiotic decay, anaerobic decay, ATR-FTIR, carbohydrates, confocal Raman imaging, erosion bacteria, lignin, Norway spruce, *Picea abies*, waterlogged archaeological wood

***Corresponding author: Nanna Bjerregaard Pedersen,** University of Copenhagen, Faculty of Science, Rolighedsvej 23, 1958 Frederiksberg C, Denmark, e-mail: nape@ign.ku.dk
**Notburga Gierlinger:** ETH Zurich, Institute of Building Materials, Stefano-Franscini-Platz 3, 8093 Zurich, Switzerland
**Lisbeth Garbrecht Thygesen:** University of Copenhagen, Faculty of Science, Rolighedsvej 23, 1958 Frederiksberg C, Denmark

DOI 10.1515/hf-2014-0024
Received January 28, 2014; accepted April 10, 2014; previously published online May 28, 2014

## Introduction

Wood is preserved for centuries or even millennia in anoxic waterlogged soils and sediments in absence of fast lignocellulose degrading microorganisms. However, microbial degradation is facilitated by erosion bacteria (EB) (Björdal et al. 1999; Kim and Singh 2000; Klaassen 2008). Typical EB decay is observed as a random mixture of sound and decayed tracheids in cross section (CS). Lignin rich cell corners (CC) and compound middle lamella (CML) are intact whereas decayed tracheids contain partly preserved S1 and S3 layers and a residual material (RM) from the decayed S2 layer (Figure 1) (Holt and Jones 1983; Singh et al. 1990; Singh and Butcher 1991; Kim et al. 1996; Björdal et al. 2000).

Anaerobic microbiological degradation of lignocellulosic materials is not fully understood. There is a lack of species description of the microorganism communities acting on the material, the enzymatic pathways are not completely surveyed, and the chemical composition of the residual wood structure is not fully elucidated (van der Lelie et al. 2012). Waterlogged archaeological wood (WAW) is well suited for studying the slow anaerobic microbiological degradation. Studies of chemical changes in this context show mainly lignin conservation and carbohydrate depletion independently of decay type, wood species, and submerging environment (Pedersen et al. 2013). However, degradation of WAW is a complex process. The characteristics of the residual wood structure depend on the composition and conformation of the biopolymers and the 3D architectural organisation. Spatially resolved chemical information at the molecular level is needed to gain in-depth insights into the decay mechanisms and residual cell wall structure. Chemical imaging

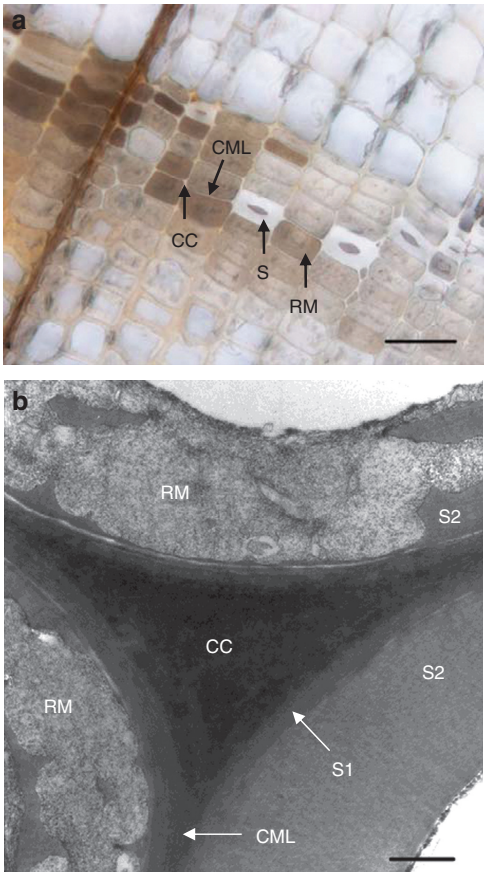


**Figure 1** Light (a) and transmission electron microscopy (b) images of waterlogged archaeological wood decayed by erosion bacteria. Sound tracheids (S/S2) are distributed among decayed. Decayed tracheids hold an amorphous residual material (RM). Cell corners (CC), compound middle lamella (CML), and S1 are intact. Scale bars=50 μm (a) and 1 μm (b).

methods are well suited for studying individual wood cell wall layers *in situ* (Fackler and Thygesen 2013).

WAW has already been studied by high resolution UV-microspectrophotometry (UMSP) (Cufar et al. 2008; Rehbein et al. 2013; Pedersen et al. 2014). UMSP permits determination of the lignin content and distribution in the cell wall with a spatial resolution of 0.25 μm×0.25 μm (Koch and Kleist 2001). The previous studies involved *Pinus sylvestris* (50–80 years), *Picea abies* (400 years), *Quercus* sp. (~4500 years), and *Fraxinus* sp. (~5200 years). All samples showed signs of EB decay (Nilsson and Klaassen 2008). The RMs of these woods contained lignin or lignin-like compounds, but the UV-absorbance images showed a great variety of lignin content in the RM. This was interpreted as lignin aggregation following EB decay (Pedersen et al. 2014). UMSP line scans of RM were similar to those of sound S2. This indicated that the chemical structure of the aromatic ring system in lignin did not change during EB decay; depolymerisation of lignin could however not be ruled out.

Confocal Raman imaging (CRI) is another imaging technique suitable for studying plant materials *in situ*. The method makes it possible to study changes in chemistry and microfibril orientation in cell wall layers with a spatial resolution higher than 0.5 μm (Agarwal 2006; Gierlinger and Schwanninger 2007; Richter et al. 2011; Gierlinger et al. 2012). Highly polar bonds such as in water have weak Raman intensities, and do not interfere with the Raman spectrum of wood (Wiley and Atalla 1987; Gierlinger and Schwanninger 2007). The method is therefore highly relevant for WAW which can be sampled without any dehydration of the material. On the other hand, the interpretation of Raman images and underlying Raman spectra is not straight forward because of the overlapping bands of cellulose, hemicelluloses, lignin, and pectin (Gierlinger et al. 2012). Hemicelluloses and cellulose have similar types of chemical bonds, while the former have broader bands and lower signal intensities than the latter. Thus the contribution of hemicelluloses is hidden. But characteristic bands of lignin do not overlap with those of polysaccharides (Agarwal and Ralph 1997). Therefore, the contribution of these two essential cell wall polymers can be well distinguished by CRI *in situ*.

The present work apply CRI to study the decay pattern of lignocelluloses in WAW poles (Norway spruce) solely decayed by EB under anoxic conditions. The aim is to get detailed spatially resolved information on the distribution and molecular structure of both lignin and carbohydrates in WAW. Attenuated total reflection Fourier transform infrared spectroscopy (ATR-FTIR) will also be applied for comparison and complementary information.

## Material and methods

The used sample material was wood discs from the bottom part of three 400-year-old Norway spruce [*Picea abies* (L.) Karst] poles; recent Norway spruce served as reference. The waterlogged poles had most likely been standing in anoxic sediment or soil from construction until excavation in 2011. The discs were stored in tap water in individual plastic buckets, purged with nitrogen gas and sealed with an airtight lid until sample preparation and analysis. Previous microscopy studies of the WAW discs showed typical EB decay and no trace of soft rot fungi or tunnelling bacteria (Figure 1) (Pedersen et al. 2014).

CRI was performed on cross sections from the sapwood of the three WAW discs. Specimens were hand cut with razor blades in a distance of 0–5 mm or 10–15 mm from the surface of each pole with

at least one growth ring present in each specimen. The same sample regions had previously been examined with LM, TEM, and UMSP (Pedersen et al. 2014). Three specimens were taken from pole 1, and one specimen from each of pole 2 and pole 3. Two specimens were prepared from sapwood of the reference material. The specimens were placed on a microscope slide, immersed in water, covered with a cover-slip, and sealed with nail polish. The specimens were aligned under the CRI microscope so that the tangential directions were parallel to the laser polarisation. Raman spectra were acquired with a confocal Raman microscope (alpha300, WITec GmbH, Ulm, Germany) equipped with an objective [100×, oil, NA=1.25, 0.17 mm cover slip correction from Nikon Instruments (Amstelveen, The Netherlands)] and a high-precision motorized scan stage. A linear polarised laser with 532 nm wavelength (Crysta Laser, Reno, NV, USA) was focused with a diffraction limited spot size of 0.61×λ/NA. Raman light was detected with an air cooled back-illuminated charge-coupled device (CCD) detector (DV401_BV, Andor, Belfast, UK) with a spectral resolution of 6 $cm^{-1}$. It has been observed that the 1600 $cm^{-1}$ band assigned to lignin is declined in wood tissue sampled in water when exposed to an intense laser beam (Agarwal 2006). Thus the laser beam intensity was reduced to half of the power to avoid sample degradation. In addition, all specimens were observed with the same instrument parameters. Latewood areas of interest were chosen for sequential scanning of spectra of adjacent sample positions by means of the motorised stage (mapping). An integration time of 0.4 s was chosen and every pixel corresponded to one scan. One spectrum was acquired for every 0.33 µm step. Every Raman image is thus based on thousands of spectra, each being a spatially resolved molecular "fingerprint" of the cell wall.

The ScanCtrlSpectroscopy 2.08 software (WITec, Ulm, Germany) was used for the measurement setup, the spectral analysis, and the image processing. Raman images were produced with a sum filter that calculated the integrated band area intensity within the chosen wavenumber interval (linear baseline subtracted). The band at 1095 $cm^{-1}$ (1080–1190 $cm^{-1}$, CC and CO stretching of carbohydrates) was selected for imaging of the carbohydrate distribution (Wiley and Atalla 1987; Agarwal and Ralph 1997). The distribution of the lignin content was depicted based on the band at 1600 $cm^{-1}$ (1540–1720 $cm^{-1}$, aromatic ring stretching) (Agarwal and Ralph 1997). This band interval contains a bending mode for water at 1640 $cm^{-1}$ but this weak band (even in presence of pure water in the lumens) is not expected to contribute significantly to the total intensity of the lignin band. The CH and $CH_2$ stretching vibrations at 2900 $cm^{-1}$ (2840–3000 $cm^{-1}$) were used for a general view of the wood structure and the quality of the analysed specimens. To overcome artefacts caused by uneven surfaces and changes in laser intensity, ratios were constructed based on the lignin (1600 $cm^{-1}$) and carbohydrate (1095 $cm^{-1}$) bands (Hänninen et al. 2011; Gierlinger et al. 2012). However, decayed tracheids were evaluated by images constructed from the area of the chosen Raman bands rather than from peak area ratios due to massive loss of carbohydrates, which made the ratio method impracticable.

Average spectra were constructed by marking selected areas on the Raman image. Average spectra were generated on all obtained Raman images from CC areas, radial (R) and tangential (T) CML areas, sound S2 areas, S1 areas parallel to the laser light, RM areas, and RM areas with high, low, and intermediate lignin contents. Each area was a sum of as many cell wall compartment areas as possible. Summed areas varied from approximately 10 $µm^2$ (CC areas) to 1000 $µm^2$ or more (S2 and RM areas). All average Raman spectra are presented without further modification.

Sample areas for ATR-FTIR with complete EB decay (where no intact tracheids are left) and inner parts of the poles without microbiological decay were located in the three WAW discs by LM examination of hand cut cross sections with light microscope (Zeiss Axioplan, Jena, Germany). Specimens were hand cut in radial-longitudinal direction (RL) with a thickness of approximately 1 mm. Five specimens were taken from a distance of 0–2 mm from the surface in two different areas on two of the discs (10 specimens for each disc) representing xylem with complete EB decay of the S2 layer. Five specimens were taken in a distance of 30–50 mm from the surface in two different areas on all three discs (10 specimens for each disc) representing sound xylem without microbiological decay. Reference material was hand cut randomly in RL direction from *P. abies* sapwood (10 specimens) and heartwood (10 specimens). ATR-FTIR measurements were recorded on a Thermo Scientific (Waltham, MA, USA) Nicolet 6700 FT-IR, Pike Technologies GladiATR diamond spectrometer, a working temperature of 25°C in the range 4000 $cm^{-1}$ to 600 $cm^{-1}$ with 100 scans and a resolution of 4.0 $cm^{-1}$; a background was taken with 200 scans. All IR spectra were normalised by standard normal variate (SNV) transformation. This is a data pre-treatment that scales and centres each spectrum and removes light scattering effects (Barnes et al. 1989).

# Results and discussion

## Sound tracheids

CRI of reference material (Figure 2a) showed expected high levels of lignin in CC and CML and high polysaccharide contents in the secondary (S2) cell wall (Fengel 1969; Fergus et al. 1969). However, lignin in both S2 and CC may be more heterogeneously distributed than suggested by UV studies (Tirumalai et al. 1996; Singh et al. 2002; Agarwal 2006). In this context, the heterogeneity of the

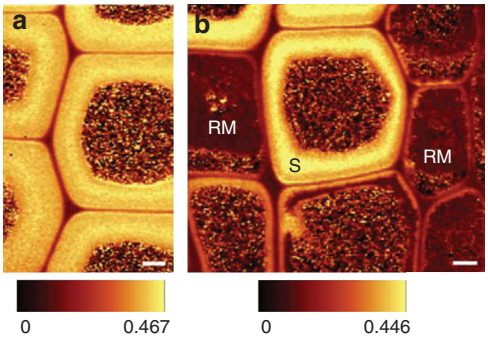


**Figure 2** Raman images of Norway spruce generated as ratios of sum filters from 1080 to 1190 $cm^{-1}$ (CC and CO stretching vibrations, carbohydrates) and from 1540 to 1720 $cm^{-1}$ (aromatic ring stretching, lignin). (a) Reference (b) waterlogged archaeological wood decayed by erosion bacteria; sound tracheids (S) have the same carbohydrate and lignin distribution as the reference. Scale bars=5 µm.

reference was moderate (Figure 2a). Sound tracheids in WAW had overall the same carbohydrate and lignin distribution as the reference (Figure 2b). This was expected based on LM, TEM and UMSP analysis of the same material (Pedersen et al. 2014) and from earlier microscopic studies of waterlogged archaeologcial wood (WAW) (Blanchette et al. 1990; Björdal et al. 2000).

## Tracheids decayed by EB

Distinct band increments assigned to lignin (1605 $cm^{-1}$, 1590 $cm^{-1}$ 1508 $cm^{-1}$, 1263 $cm^{-1}$, 1215 $cm^{-1}$, 1140 $cm^{-1}$ 1086 $cm^{-1}$, and 856 $cm^{-1}$) and band decrements assigned to carbohydrates (1732 $cm^{-1}$, 1307 $cm^{-1}$, 1095 $cm^{-1}$, 1050 $cm^{-1}$, 1024 $cm^{-1}$, and 895 $cm^{-1}$) were seen in ATR-FTIR spectra of heavily decayed WAW xylem from the outermost growth rings compared to the reference (Marchessault 1962; Faix 1991; Schwanninger et al. 2004; Fackler et al. 2010) (Figure 3). This is in agreement with previous FT-IR spectroscopy studies of WAW (Pavlikova et al. 1993; MacLeod and Richards 1997; Gelbrich et al. 2008; Giachi and Pizzo 2009; Petrou et al. 2009). Even though the analysed WAW did not have any intact S2, the carbohydrate contributions were still strong except for the band assigned to C=O stretch in unconjugated carbonyls at 1735 $cm^{-1}$ (Schwanninger et al. 2004), which was completely lost. The relatively strong carbohydrate contribution is expected to stem from polysaccharides in CML, sound S1, and fractions of S3 still present in the heavily decayed xylem.

CRI (Figure 2b) shows massive loss of carbohydrates in the RM left after S2 decay. This is the results of the preferential decay of polysaccharides in the S2 by EB (Pedersen et al. 2013). Average spectra from CRI in RM areas and sound S2 layers confirmed strong depletion of polysaccharides (Figure 4a). The band at 1095 $cm^{-1}$ (carbohydrates) was completely lost. The band at 2900 $cm^{-1}$ (CH and $CH_2$ stretching) was heavily reduced, which further confirms loss of carbohydrates. Raman spectra obtained from the WAW specimens had noisier Raman spectra than the reference (Figure 4b). This is most likely due to an increased fluorescence caused by the higher relative lignin content and/or chromophores formed in WAW. Due to the high fluorescence, the polysaccharide bands in WAW were expected to be less resolved. On the other hand, sound cell wall areas in WAW had polysaccharide band intensities (1095 $cm^{-1}$ and 2900 $cm^{-1}$) comparable to the reference (Figure 4b). Thus the polysaccharide depletion in the RM of decayed tracheids can be ascribed to EB decay.

CRI constructed as sum filters from 1080 to 1190 $cm^{-1}$ (carbohydrates) also showed very low carbohydrate content in the RM (Figure 5a). The carbohydrate content was less than observed in CML and in some CC areas. This is a sign of effective polysaccharide degradation by EB. However, a few small areas with carbohydrate levels as high as in sound S2 were also observed (Figure 5a). These areas were interpreted as un-decayed fractions of S3, as such fractions have been observed previously by TEM (Pedersen et al. 2014). The tangential CMLs showed

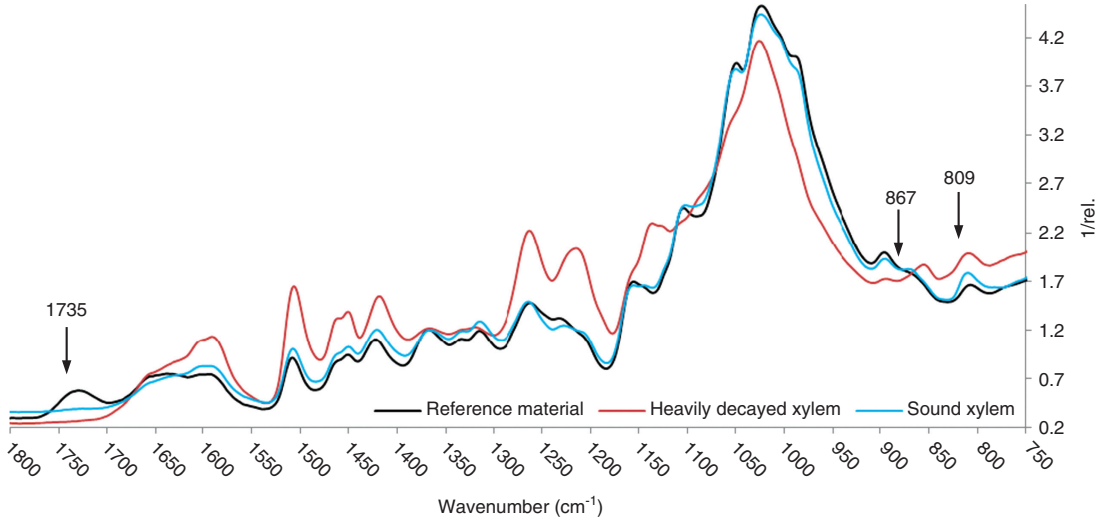


**Figure 3** Average ATR-FTIR spectra of sound waterlogged archaeological spruce xylem, of heavily decayed surface layers of spruce xylem, and of reference. Band positions for unconjugated C=O stretching in acetyl groups in glucomannan and ester linkages in the carbohydrate lignin complex (1735 $cm^{-1}$) and for the glucomannan backbone (867 and 809 $cm^{-1}$) are indicated with arrows.

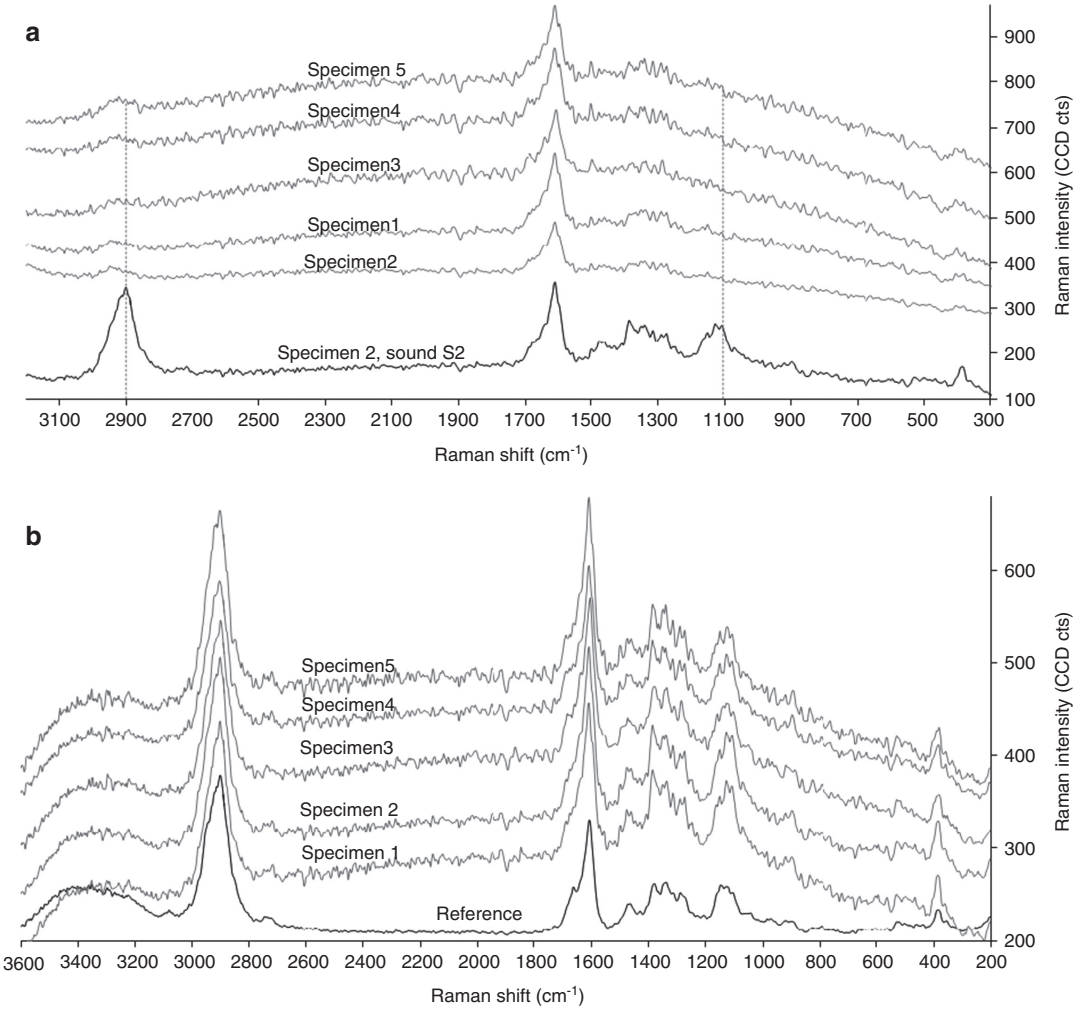


**Figure 4** Average Raman spectra of (a) residual material (RM) and of (b) sound S2 in waterlogged archaeological spruce in five different specimens (grey lines) compared to a spectrum of either sound S2 (a) or S2 in reference (b) (black lines). (a) RM show total lack of carbohydrates contributions (1095 $cm^{-1}$ and 2900 $cm^{-1}$, dotted lines) (b) Spectra of sound S2 in waterlogged spruce show minor spectral changes compared to reference (1600 $cm^{-1}$ and 1100 $cm^{-1}$).

in general higher Raman intensities of the carbohydrate bands than those of the radial CML (Figure 5a). This is not due to concentration differences, but to the various microfibril orientations in T and R oriented cell walls in the preserved S1 layer relative to the laser polarisation. Changing the laser polarization from parallel (0°) to perpendicular (90°) to the microfibril angle (MFA) in cross sections leads to large changes in the Raman intensity of almost all characteristic bands (Agarwal and Atalla 1986; Gierlinger et al. 2010; Thygesen and Gierlinger 2013).

Images constructed as sum filters from 1540 to 1720 $cm^{-1}$ (aromatic ring stretching; Figure 5b) showed a better distinction between RM and empty lumen areas, and a more varied distribution of lignin in the RM compared to images constructed as band ratios (Figure 5c). The lignin distribution images showed that all decayed tracheids contained RM with high, intermediate, and low levels of aromatic compounds within the same tracheids (Figure 5b). These lignin concentrations corresponded to normal levels in CML, normal levels in sound S2, and lower levels than seen in sound S2, respectively. This lignin distribution pattern was also observed with UMSP of the same sample material (Pedersen et al. 2014). The Raman data demonstrated that the uneven lignin distribution in the RM is not an artefact due to sample modification (e.g., embedding in Spurr's resin for UMSP measurements), as the sampling for CRI does not need dehydration or embedding in a resin.

The lignin contribution in FT-IR spectra of EB degraded WAW was much stronger than in the reference, but no band broadening was observed. The Raman band at 1600 $cm^{-1}$ (aromatic ring stretching) revealed different

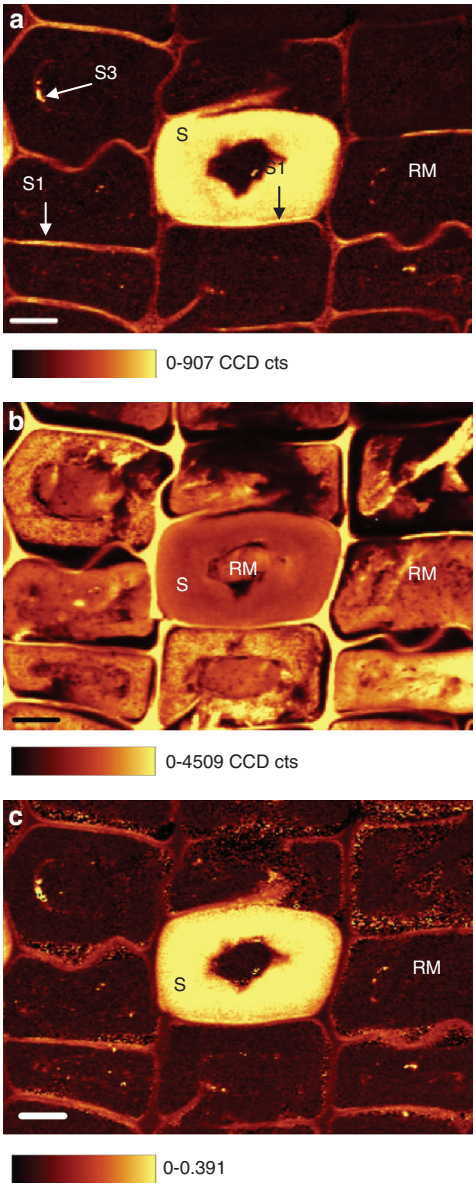


**Figure 5** Raman images of one waterlogged archaeological wood specimen decayed by erosion bacteria generated as sum filters from 1080 to 1190 $cm^{-1}$ (carbohydrates) (a) and 1540 to 1720 $cm^{-1}$ (lignin) (b). Or generated as a ratio of sum filters from 1080 to 1190 $cm^{-1}$ and 1540 to 1720 $cm^{-1}$ (c). One sound tracheid (S) is surrounded by decayed tracheids that contain residual material (RM) with variable levels of lignin (b) but no signal from carbohydrates (a and c); the sound tracheid contains RM due to decay situated elsewhere in the tracheid. Remnants of S3 and S1 can be detected (a). Scale bar=10 µm.

intensities for the RM but no band broadening, evolvement of new shoulders, or any band shifts compared to sound S2 in WAW (Figure 6). This indicates that the chemical composition of lignin in the S2 did not change due to EB decay. However, depolymerisation of lignin cannot be ruled out.

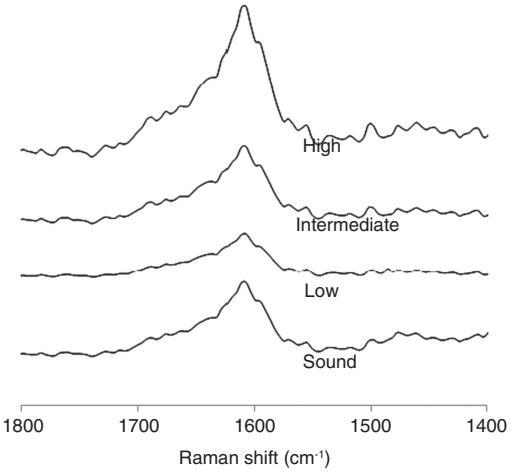


**Figure 6** Average Raman spectra of residual material with high, low, and intermediate levels of aromatic ring stretching contributions in the band area assigned to lignin (1600 $cm^{-1}$) compared to sound S2. The lignin bands do not show any band broadening but merely a difference in intensity.

## Abiotic decay in morphologically sound xylem

Average Raman spectra of morphologically sound cell wall compartments (CC, CML, S2, and S1) in WAW showed small spectral differences compared to those of the reference (Figure 4b). ATR-FTIR analysis of sound WAW xylem confirmed that minor chemical changes had occurred in areas free from microbiological decay compared to the reference (Figure 3). The cell walls were morphologically intact and the chemical changes must therefore be assigned to abiotic decay as a consequence of waterlogging for 400 years.

In ATR-FTIR spectra of sound xylem, the band at 1735 $cm^{-1}$ was completely lost, as was seen in heavily decayed xylem (Figure 3). The band is assigned to C=O stretch in unconjugated carbonyls (Schwanninger et al. 2004) or more limited to C=O stretching of acetyl or carboxylic acid in hemicelluloses (Marchessault 1962). Complete loss of the band at 1735 $cm^{-1}$ has been observed earlier in WAW and has in some cases been ascribed to degradation of hemicelluloses (Kim 1990; Wilson et al. 1993; MacLeod and Richards 1997; Giachi and Pizzo 2009; Sandak et al. 2010). Band positions for unconjugated carbonyl groups are in the range from 1810 to 1690 $cm^{-1}$ with esters giving the best match at 1735 $cm^{-1}$ (Pavia et al. 2009). Un-conjugated carbonyl groups are not present in softwood lignin in significant amounts (Brunow and Lundquist 2010). In softwood hemicelluloses, esters are mainly acetyl groups in galactoglucomannans and in lignin-carbohydrate complexes between the carboxylic

acid groups in glucopyranosyluronic acid side chains of heteroxylans and OH groups of lignin (Balakshin et al. 2007; Harris and Stone 2008; Balakshin et al. 2011). Consequently, the band can be assigned to carbonyl groups in side groups of hemicelluloses. The FTIR spectrum shows indeed larger contribution from glucomannan at 867 $cm^{-1}$ and 809 $cm^{-1}$ (Marchessault 1962) in WAW compared to reference (Figure 3). Accordingly, the glucomannan backbone was preserved but the acetyl groups lost. This finding is supported by a study by Pan et al. (1990) on 6600 years old waterlogged intact hardwood (*Bischofia polycarpa*). $^{13}C$ NMR analyses on milled wood lignin (MWL) from the WAW showed that the remaining hemicellulose fraction did not contain any O-acetyl groups, which was believed to be caused by slow *in situ* hydrolysis of the acetyl groups to acetic acid. The enhanced acidity that results from this process has the potential to depolymerise the biopolymers by catalysing hydrolysis of glycosidic bonds in polysaccharides and ether bonds in lignin. The process is believed to be very slow for the material studied here due to low temperature, low concentration of acetic acid, relatively high $pK_a$ of acetic acid, and steric hindrance in the solid lignocellulosic material. It is not clear to which degree xylan was degraded apart from the loss of ester linkages. Splitting ester linkages within the lignin-carbohydrate complex should lead to a weakening of the cell wall though the microfibrils remain intact. This is consistent with observations by Borgin et al. (1975). In Raman spectra, bands of hemicelluloses are not clearly visible as they are overlapping with cellulose bands (Agarwal and Ralph 1997). However, small spectral changes are observed in Raman spectra of sound S2 compared to the reference around 1100 $cm^{-1}$ and 2900 $cm^{-1}$ (Figure 4b). This supports the observed modification of hemicelluloses from the ATR-FTIR analysis.

The spectral fingerprint of the Raman band at 1600 $cm^{-1}$ (lignin) is identical in sound cell wall compartments and in RM of WAW, but slightly different to that of the reference (Figure 7a). This indicates small abiotic modifications of the lignin due to the waterlogged environment. All five WAW specimens feature several shoulders that were not observed in the reference. Comparing the different sound cell wall compartments (S2, S1, CC, and R and T CML) in individual specimens showed unchanged spectral fingerprint for the aromatic ring stretching region (Figure 7b). The more noisy character of the WAW Raman spectra has to be taken into consideration. Nevertheless, it is striking that four specimens (specimen 1, 2, 4, 5) of the five show the same trends. The aromatic ring stretching at 1607 $cm^{-1}$ and 1664 $cm^{-1}$ appear at the same wavenumber but shoulders at approximately 1555, 1571, 1595, 1628, 1644, 1676, and

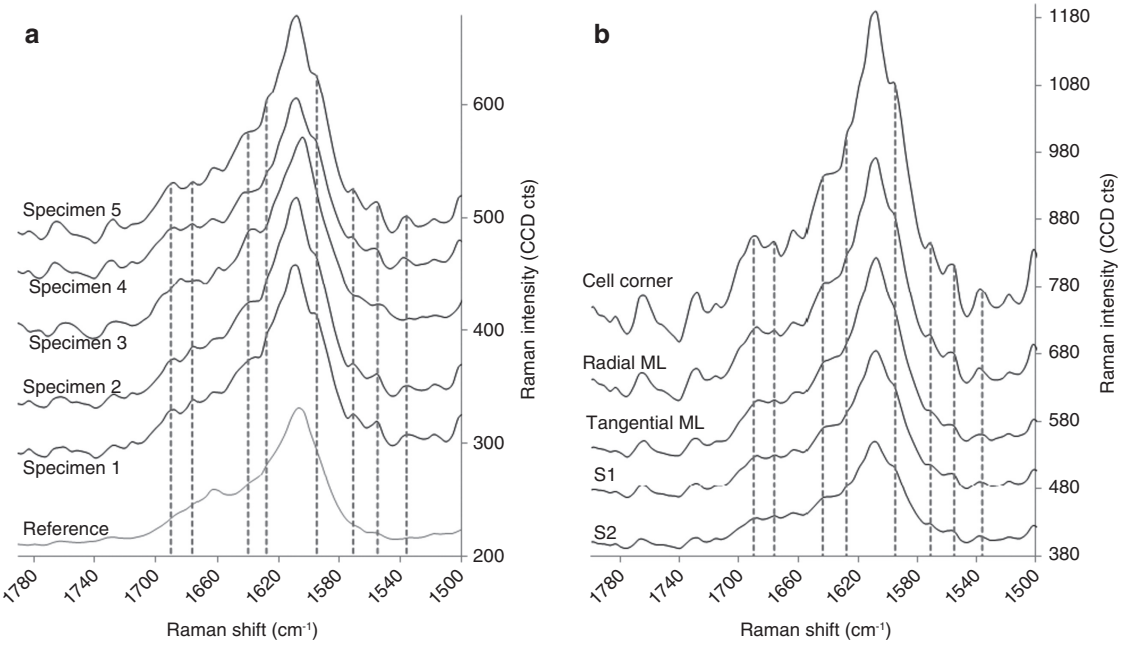


**Figure 7** Average Raman spectra in the band area assigned to lignin (1600 $cm^{-1}$). (a) Sound S2 in five waterlogged archaeological wood specimens and in reference material (detail of spectrum in Figure 5); shoulders that are not present in reference is shown with vertical dashed lines. (b) Sound cell wall compartments of specimen 4; all shoulders in the 1600 $cm^{-1}$ band area are identical in all cell wall compartments.

**Table 1** Raman bands assigned to oxidation of lignin collected from the literature.

| Band ($cm^{-1}$) | Assigned to | Material |
|---|---|---|
| 1125 | Conifer aldehyde, conifer alcohol structures[a] | TMP spruce |
| 1316 | Oxidation product from lignin[b]/conjugated C=C[c] | TMP spruce/model compounds |
| 1400 | Oxidation product from lignin[b] | TMP spruce |
| 1473 | Conjugated C=C[c] | Model compounds |
| 1498 | Condensed structures[c] | Model compounds |
| 1518 | Gyaiacyl[c] | Model compounds |
| 1539 | Oxidation product from lignin[b]/conjugated C=C[c] | TMP spruce/model compounds |
| 1555 | *o*-quinone[d]/condensed structures[c] | TMP spruce/model compounds |
| 1571 | Degradation product from heat treatment[e] | Scots pine |
| 1595 | Conifer aldehyde[f,g]/oxidation product from lignin[b] | TMP spruce |
| 1620 | Condensed structures[c] | Model compounds |
| 1628 | Conifer aldehyde[d,g]/methyl hydroquinone[f]/γ-carbonyl marker band[b] | TMP spruce |
| 1644 | *p*-quinone[d] | TMP spruce |
| 1676 | *p*-quinone[d]/conjugated C=O[c] | TMP spruce/model compounds |
| 1690 | Conjugated C=O[c] | Model compounds |

[a]Agarwal and McSweeny (1997).
[b]Vester et al. (2004).
[c]Saariaho et al. (2005).
[d]Agarwal (1998).
[e]Nuopponen et al. (2004).
[f]Agarwal (2008).
[g]Agarwal and Ralph (2008).

1690 $cm^{-1}$ emerged in the WAW. Specimen 3 was regarded as an outlier since this specimen is from the same pole as specimens 1 and 2. Based on the literature concerning photochemically or enzymatically oxidised or heat treated wood or thermo mechanical pulp (TMP) presented in Table 1, it can be concluded that lignin is most likely oxidised in WAW to structures such as conifer aldehyde, conjugated C=C, conjugated C=O, *o*-quinone, and *p*-quinone (Pandey and Vuorinen 2008). Comprehensive oxidation of aromatic rings will lower and broaden the 1600 band $cm^{-1}$ and give rise to spectral changes in the 1500–1000 $cm^{-1}$ range as a consequence of degradation products (Agarwal and McSweeny 1997; Pandey and Vuorinen 2008). However, this is not the case for the WAW but could be explained by the fact that the cell walls of the WAW are morphologically intact; de-polymerisation has not occurred within the lignocellulosic matrix of the cell wall at this initial stage of oxidation.

## Conclusion

CRI of waterlogged archaeological wood (WAW) *P. abies* found as poles submerged under anoxic condition for approximately 400 years and solely decayed by EB confirmed that decayed tracheids hold a lignin containing RM and that the distribution of lignin varies within the same tracheid from lower levels than seen in sound S2 to levels as high as in the CML. Raman spectra show that the chemical composition of the lignin in the RM do not differ from intact S2. However, the RM reveals strong depletion of carbohydrates indicating an effective carbohydrate metabolism by EB. Evidence for abiotic decay due to waterlogging was found in intact xylem free from microbiological decay. ATR-FTIR spectra showed complete loss of acetyl groups in hemicelluloses and loss of ester linkages, probably from lignin-carbohydrate complexes, whereas Raman spectra revealed minor oxidation of the lignin polymer.

**Acknowledgments:** Nanna Bjerregaard Pedersen would like to thank COST Action FP0802 for supporting the work as a Short Term Scientific Mission. We thank Institute of Polymer Science, Johannes Kepler University, Linz, Austria for hosting the experiments and Museum of Copenhagen for donation of the test material.

## References

Agarwal, U.P. (1998) Assignment of the photoyellowing-related 1675 $cm^{-1}$ Raman/IR band to p-quinones and its implications to the mechanism of color reversion in mechanical pulps. J. Wood Chem. Technol. 18:381–402.

Agarwal, U.P. (2006) Raman imaging to investigate ultrastructure and composition of plant cell walls: distribution of lignin and cellulose in black spruce wood (*Picea mariana*). Planta 224:1141–1153.

Agarwal, U.P. (2008) Raman spectroscopic characterization of wood and pulp fibers. In: Characterization of Lignocellulosic Materials. Blackwell Publishing Ltd., Oxford, UK. pp. 17–35.

Agarwal, U.P., Atalla, R.H. (1986) In-situ Raman microprobe studies of plant cell walls: Macromolecular organization and compositional variability in the secondary wall of *Picea mariana* (Mill.) B.S.P. Planta 169:325–332.

Agarwal, U.P., McSweeny, J.D. (1997) Photoyellowing of thermomechanical pulps: looking beyond alpha-carbonyl and ethylenic groups as the initiating structures. J. Wood Chem. Technol. 17:1–26.

Agarwal, U.P., Ralph, S.A. (1997) FT-Raman spectroscopy of wood: identifying contributions of lignin and carbohydrate polymers in the spectrum of black spruce (*Picea mariana*). Appl. Spectrosc. 51:1648–1655.

Agarwal, U.P., Ralph, S.A. (2008) Determination of ethylenic residues in wood and TMP of spruce by FT-Raman spectroscopy. Holzforschung 62:667–675.

Balakshin, M.Y., Capanema E.A., Chang, H.-M. (2007) MWL fraction with a high concentration of lignin-carbohydrate linkages: isolation and 2D NMR spectroscopic analysis. Holzforschung 61:1–7.

Balakshin, M., Capanema, E., Gracz, H., Chang, H.-M., Jameel, H. (2011) Quantification of lignin-carbohydrate linkages with high-resolution NMR spectroscopy. Planta 233:1097–1110.

Barnes, R.J., Dhanoa, M.S., Lister, S.J. (1989) Standard normal variate transformation and de-trending of near-infrared diffuse reflectance spectra. Appl. Spectrosc. 43:772–777.

Björdal, C.G., Nilsson, T., Daniel, G. (1999) Microbial decay of waterlogged archaeological wood found in Sweden applicable to archaeology and conservation. Int. Biodeter. Biodegr. 43:63–73.

Björdal, C.G., Daniel, G., Nilsson, T. (2000) Depth of burial, an important factor in controlling bacterial decay of waterlogged archaeological poles. Int. Biodeter. Biodegr. 45:15–26.

Blanchette, R.A., Nilsson, T., Daniel, G. Abad, A. (1990) Biological degradation of wood. In: Archaeological Wood. Properties, Chemistry, and Preservation. Eds. Rowell, R.M., Barbour, R.J. American Chemical Society, Washington, DC. pp. 141–174.

Borgin, K., Parameswaran, N., Liese, W. (1975) The effect of aging on the ultrastructure of wood. Wood Sci. Technol. 9:87–98.

Brunow, G., Lundquist, K. (2010) Functional groups and bonding patterns in lignin (including the lignin-carbohydrate complexes). In: Lignin and Lignans. Advances in Chemistry. Eds. Heitner, C., Dimmel, D.R., Schmidt, J.A. CRC Press, Boca Raton, FL. pp. 267–299.

Cufar, K., Gricar, J., Zupancic, M., Koch, G., Schmitt, U. (2008) Anatomy, cell wall structure and topochemistry of waterlogged archaeological wood aged 5,200 and 4,500 years. IAWA J. 29:55–68.

Fackler, K., Thygesen, L.G. (2013) Microspectroscopy as applied to the study of wood molecular structure. Wood Sci. Technol. 47:203–222.

Fackler, K., Stevanic, J.S., Ters, T., Hinterstoisser, B., Schwanninger, M., Salmen, L. (2010) Localisation and characterisation of incipient brown-rot decay within spruce wood cell walls using FT-IR imaging microscopy. Enzyme Microb. Technol. 47:257–267.

Faix, O. (1991) Classification of lignins from different botanical origins by FT-IR spectroscopy. Holzforschung 45:21–27.

Fengel, D. (1969) Ultrastructure of cellulose from wood. 1. Wood as basic material for isolation of cellulose. Wood Sci. Technol. 3:203–217.

Fergus, B.J., Procter, A.R., Scott, J.A.N., Goring, D.A.I. (1969) The distribution of lignin in sprucewood as determined by ultraviolet microscopy. Wood Sci. Technol. 3:117–138.

Gelbrich, J., Mai, C., Militz, H. (2008) Chemical changes in wood degraded by bacteria. Int. Biodeter. Biodegr. 61:24–32.

Giachi, G., Pizzo, B. (2009) A chemical characterisation of the decay of waterlogged archaeological wood. In: Proceedings of the 10th ICOM Group on Wet Organic Archaeological Materials Conference, Amsterdam 2007. Eds. Strætkvern, K., Huisman, D.J. Rijksdienst voor Archaeologie, Cultuurlandschap en Monumenten, Amersfoort. pp. 21–33.

Gierlinger, N., Schwanninger, M. (2007) The potential of Raman microscopy and Raman imaging in plant research. Spectroscopy 21:69–89.

Gierlinger, N., Luss, S., König, C., Konnerth, J., Eder, M., Fratzl, P. (2010) Cellulose microfibril orientation of *Picea abies* and its variability at the micron-level determined by Raman imaging. J. Exp. Bot. 61:587–595.

Gierlinger, N., Keplinger, T., Harrington, M. (2012) Imaging of plant cell walls by confocal Raman microscopy. Nat. Prot. 7: 1694–1708.

Hänninen, T., Kontturi, E., Vuorinen, T. (2011) Distribution of lignin and its coniferyl alcohol and coniferyl aldehyde groups in *Picea abies* and *Pinus sylvestris* as observed by Raman imaging. Phytochemistry 72:1889–1895.

Harris, P.J., Stone, B.A. (2008) Chemistry and molecular organization of plant cell walls. In: Biomass Recalcitrance. Deconstructing the Plant Cell Wall for Bioenergy. Ed. Himmel, M.E. Blackwell Publishing, Oxford. pp. 61–93.

Holt, D.M., Jones, E.B. (1983) Bacterial degradation of lignified wood cell walls in anaerobic aquatic habitats. Appl. Environ. Microbiol. 46:722–727.

Kim, Y.S. (1990) Chemical characteristics of waterlogged archaeological wood. Holzforschung 44:169–172.

Kim, Y.S., Singh, A.P. (2000) Micromorphological characteristics of wood biodegradation in wet environments: a review. IAWA J. 21:135–155.

Kim, Y.S., Singh, A.P., Nilsson, T. (1996) Bacteria as important degraders in waterlogged archaeological woods. Holzforschung 50:389–392.

Klaassen, R.K.W.M. (2008) Bacterial decay in wooden foundation piles – patterns and causes: a study of historical pile foundations in the Netherlands. Int. Biodeter. Biodegr. 61:45–60.

Koch, G., Kleist, G. (2001) Application of scanning UV microspectrophotometry to localise lignins and phenolic extractives in plant cell walls. Holzforschung 55:563–567.

MacLeod, I.D., Richards, V.L. (1997) Wood degradation on historic shipwreck sites: the use of FT-IR spectroscopy to study the loss of hemicellulose. In: Proceedings of the 6th ICOM Group on Wet Organic Archaeological Materials Conference, York 1996. Eds. Hoffmann, P., Grant, T., Spriggs, J.A., Daley, T. The International Council of Museums (ICOM), Bremerhaven. pp. 203–225.

Marchessault, R.H. (1962) Application of infra-red spectroscopy to cellulose and wood polysaccharides. In: Pure and Applied

Chemistry. Wood Chemistry Symposium, Montreal, Canada, 9–11 August 1961, pp. 107–129.
Nilsson, T., Klaassen, R.K.W.M. (2008) Abiotic or bacterial degradation? IAWA J. 29:336–338.
Nuopponen, M., Vuorinen, T., Jamsa, S., Viitaniemi, P. (2004) Thermal modifications in softwood studied by FT-IR and UV resonance Raman spectroscopies. J. Wood Chem. Technol. 24:13–26.
Pan, D.R., Tai, D.S., Chen, C.L., Robert, D. (1990) Comparative-studies on chemical-composition of wood components in recent and ancient woods of *Bischofia-polycarpa*. Holzforschung 44:7–16.
Pandey, K.K., Vuorinen, T. (2008) Comparative study of photodegradation of wood by a UV laser and a xenon light source. Polym. Degrad. Stabil. 93:2138–2146.
Pavia, D.L., Lampman, G.M., Kriz, G.S., Vyvyan, J.R. Introduction to Spectroscopy. Brooks/Cole, Belmont, CA, USA, 2009.
Pavlikova, H., Sykorova, I., Cerny, J., Sebestova, E., Machovic, V. (1993) Spectroscopic study of degraded woods from the Elbe river valley. Energy Fuels 7:351–356.
Pedersen, N.B., Björdal, C.G., Jensen, P., Felby, C. (2013) Bacterial degradation of archaeological wood in anoxic waterlogged environments. In: Stability of Complex Carbohydrate Structures. Biofuel, Foods, Vaccines and Shipwrecks. Ed. Harding, S.E. The Royal Society of Chemistry, Cambridge. pp. 160–187.
Pedersen, N.B., Schmitt, U., Koch, G., Felby, C., Thygensen, L.G. (2014) Lignin distribution in waterlogged archaeological *Picea abies* (L.) Karst degraded by erosion bacteria. Holzforschung 68:791–798 .
Petrou, M., Edwards, H.G.M., Janaway, R.C., Thompson, G.B., Wilson, A.S. (2009) Degradation of Neolithic waterlogged pine and oak timbers from northern Greece. In: Proceedings of the 10th ICOM Group on Wet Organic Archaeological Materials Conference, Amsterdam 2007. Eds. Strætkvern, K., Huisman, D.J. Rijksdienst voor Archaeologie, Cultuurlandschap en Monumenten, Amersfoort. pp. 57–67.
Rehbein, M., Koch, G., Schmitt, U., Huckfeldt, T. (2013) Topochemical and transmission electron microscopic studies of bacterial decay in pine (*Pinus sylvestris* L.) harbour foundation piles. Micron 44:150–158.
Richter, S., Müssig, J., Gierlinger, N. (2011) Functional plant cell wall design revealed by the Raman imaging approach. Planta 233:763–772.
Saariaho, A.M., Argyropoulos, D.S., Jaaskelainen, A.S., Vuorinen, T. (2005) Development of the partial least squares models for the interpretation of the UV resonance Raman spectra of lignin model compounds. Vibrat. Spectrosc. 37:111–121.
Sandak, A., Sandak, J., Zborowska, M., Pradzynski, W. (2010) Near infrared spectroscopy as a tool for archaeological wood characterization. J. Archaeol. Sci. 37:2093–2101.
Schwanninger, M., Rodrigues, J.C., Pereira, H., Hinterstoisser, B. (2004) Effects of short-time vibratory ball milling on the shape of FT-IR spectra of wood and cellulose. Vibrat. Spectrosc. 36:23–40.
Singh, A.P., Butcher, A.J. (1991) Bacterial degradation of wood cell walls: a review of degradation patterns. J. Inst. Wood Sci. 12:143–157.
Singh, A.P., Nilsson, T., Daniel, G.F. (1990) Bacterial attack of *Pinus sylvestris* wood under near anaerobic conditions. J. Inst. Wood Sci. 11:237–249.
Singh, A., Daniel, G., Nilsson, T. (2002) Ultrastructure of the S-2 layer in relation to lignin distribution in *Pinus radiata* tracheids. J. Wood Sci. 48:95–98.
Thygesen, L.G., Gierlinger, N. (2013) The molecular structure within dislocations in *Cannabis sativa* fibres studied by polarised Raman microspectroscopy. J. Struct. Biol. 182:219–225.
Tirumalai, V.C., Agarwal, U.P., Obst, J.R. (1996) Heterogeneity of lignin concentration in cell corner middle lamella of white birch and black spruce. Wood Sci. Technol. 30:99–104.
van der Lelie, D., Taghavi, S., McCorkle, S.M., Li, L.L., Malfatti, S.A., Monteleone, D., Donohoe, B.S., Ding, S.Y., Adney, W.S., Himmel, M.E., Tringe, S.G. (2012) The metagenome of an anaerobic microbial community decomposing poplar wood chips. PLoS One 7:1–16.
Vester, J., Felby, C., Nielsen, O.F., Barsberg, S. (2004) Fourier transform Raman difference spectroscopy for detection of lignin oxidation products in thermomechanical pulp. Appl. Spectrosc. 58:404–409.
Wiley, J.H., Atalla, R.H. (1987) Band assignments in the Raman spectra of celluloses. Carbohydr. Res. 160:113–129.
Wilson, M.A., Godfrey, I.M., Hanna, J.V., Quezada, R.A., Finnie, K.S. (1993) The degradation of wood in old Indian Ocean shipwrecks. Org. Geochem. 20:599–610.